Defect Spectroscopy and Determination of the Electron Diffusion Length in Single Crystal Diamond by Total Photoelectron Yield spectroscopy

J. Ristein, W. Stein, and L. Ley

Institut f. Techische Physik, Universität Erlangen-Nürnberg, Erwin-Rommel-Strasse 1, D-91058 Erlangen, Germany

(Received 16 July 1996)

Novel photoelectron yield experiments performed with a dynamical range of 8 orders of magnitude reveal a new excitation channel for electron emission on diamond (100) and (111) surfaces with negative electron affinity which is due to defect states 2.0 and 4.1 eV below the conduction band minimum. Analyzing the competition of free conduction band electrons excited out of defects and excitons with respect to final photoelectron production we determine that the electron diffusion length in *p*-type IIb diamond is between 150 and 250 μm. [S0031-9007(97)02518-0]

PACS numbers: 79.60.Bm, 73.50.Gr

It is a special property of diamond surfaces to exhibit true negative electron affinity (NEA) when saturated by hydrogen. Under this condition the conduction band minimum (CBM) lies in energy above the vacuum level and thus NEA enables the emission of electrons from the conduction band minimum into the vacuum without the need to overcome an energy barrier. Using the shape of the inelastic peak in photoemission spectra as a qualitative criterion, NEA has been found on (111) [1] as well as on (100) surfaces [2].

In a recent series of experiments Bandis and Pate studied the photoelectron yield of natural diamond (111) surfaces as a function of photon energy [3,4]. Their most remarkable result was that the threshold for electron emission on surfaces exhibiting NEA coincides with the excitation energy of excitons which are bound by 80 meV in diamond and can obviously break up at the surface and emit an electron. In certain cases the exciton absorption is even more effective in providing photoelectrons than the absorption processes leading directly to free electron-hole pairs. Bandis and Pate attributed this to an upward band bending at their diamond (111) surface which effectively prevented electrons at the CBM to reach the surface. In this Letter we present new photoelectron yield spectra on diamond (111) and (100) surfaces exhibiting NEA. By extending the spectral range to $2.0 \ldots 6.2$ eV and the dynamical range of this method to 8 orders of magnitude new sub-band-gap features have been resolved. This increase in sensitivity was achieved by using an optical double monochromator with a straylight reduction better than 10^{-8} and an optimized electron optics with a collection efficiency for the photoelectrons which is close to unity. Details of the experimental setup are given in [5]. A quantitative analysis of the yield spectra allows the extraction of the diffusion length for electrons and an upper limit for that of the excitons which contribute to the yield.

Two type IIb single crystal diamond samples with (111) and (100) oriented surfaces were studied after they had been hydrogenated at 860 °C for 10 min in a microwave plasma. This treatment produces atomically flat, hydrogen saturated surfaces [6,7] and both samples revealed a sharp LEED pattern with very low background [(1×1) for the (111) and (2×1) for the (100) sample] after the microwave preparation. The absence of surface states in the ultraviolet excited photoemission spectra (UPS) of both samples confirmed their saturation by hydrogen. X-ray excited photoemission revealed no contaminants on the surface except for traces of oxygen (2%) and using angle resolved UPS we determined the surface Fermi level to lie 0.9 ± 0.2 eV above the valence band edge in both samples. The concentration of boron acceptors in both samples was determined by IR spectroscopy using the calibration factor of Wedepohl [8] and gave 8×10^{15} cm^{-3} for the (100) and 2×10^{16} cm^{-3} for the (111) crystal.

Before presenting experimental results the special conditions of photoelectron emission from NEA surfaces shall be briefly reviewed and compared to the more common situation of positive electron affinity (PEA). After photoexcitation electrons in the conduction band of a semiconductor will dissipate their excess kinetic energy by inelastic scattering with other electrons and phonons. This thermalization process takes place on a subpicosecond time scale and within a spatial range corresponding to the thermalization length λ of the order of 100 Å. In the case of PEA thermalized electrons at the CBM are lost for the photoemission current since they will not be able to overcome the energy barrier, the electron affinity χ, at the surface. The probe depth of the total yield technique is thus limited by λ. As long as the absorption constant α fulfills $\alpha^{-1} \gg \lambda$, which is a valid approximation near the absorption threshold, most of the photoexcited electrons will not contribute to the photoelectron current.

The situation is different for surfaces with NEA ($\chi < 0$). Thermalized electrons will now also contribute to the photoemission process and electrons are only lost by recombination which takes place on a microsecond time scale depending on the concentration of deep defect states acting as recombination centers. The escape depth is no longer limited by the thermalization length λ but instead

by the much longer diffusion length L of the electrons: The photoelectric yield will be correspondingly higher than in the case of PEA. The total yield measured at a photon energy $h\nu$ is defined as the ratio of the photoelectron current divided by the photon flux incident on the sample (and corrected for reflection losses). For a photon flux density j_0 an exponential excitation profile

$$g(x) = j_0 \alpha(h\nu) \exp[-\alpha(h\nu)x] \quad (1)$$

for the generation rate g of electrons results. When the one dimensional diffusion equation for an ensemble of electrons excited at a depth x below the surface is solved for a semi-infinite solid the probability w for reaching the surface and exiting into vacuum is given by [9]

$$w(x) = \frac{S_{\mathrm{em}}}{S_{\mathrm{em}} + S_{\mathrm{rec}} + L^{-1}D} \exp(-L^{-1}x), \quad (2)$$

where D is the electron diffusion constant, L the electron diffusion length, S_{rec} the surface recombination velocity, and S_{em} a corresponding surface transition velocity for the emission as a photoelectron which takes into account quantum mechanical reflection. Integrating $g(x) \cdot w(x)$ and normalizing to the photon flux density j_0 finally gives the total photoelectron yield for the case of NEA:

$$Y(h\nu) = \frac{p \cdot L \cdot \alpha(h\nu)}{1 + L\alpha(h\nu)}, \quad (3)$$

where $\alpha(h\nu)$ is the absorption constant and p has been used as an abbreviation for the prefactor of the exponential in Eq. (2). For those electrons which are not fully thermalized when reaching the surface p and L will depend on their original excitation energy and thus on $h\nu$. As long as $L \gg \lambda$, however, the vast majority of photoelectrons will have lost their excitation memory and L and p can be assumed constant. The variation of the total yield thus reflects directly that of the absorption constant and will be proportional to it as long as $\alpha(h\nu) \ll L^{-1}$, i.e., as long as the absorption is sufficiently weak.

In Fig. 1 we present the total yield spectra of hydrogenated diamond (111) and (100) surfaces for photon energies between 2.0 and 6.2 eV. Note the logarithmic scale of the ordinate. The spectral range is divided into three regions according to the dominating absorption processes that contribute to the photoelectron yield. Diamond is an indirect semiconductor with a band gap of 5.470 eV (at room temperature). The fundamental absorption edge for the effective production of free electron-hole pairs lies at 5.615 eV, i.e., a TO-phonon energy above the band gap [10]. Above this energy the onset of free electron emission into vacuum leads to the superlinear increase of the yield in region III. This is direct evidence for NEA after microwave hydrogenation in our samples. In region II, between 5.26 and 5.615 eV photon energy, excitonic absorption with its phonon side bands takes place and we shall return to its energy range below.

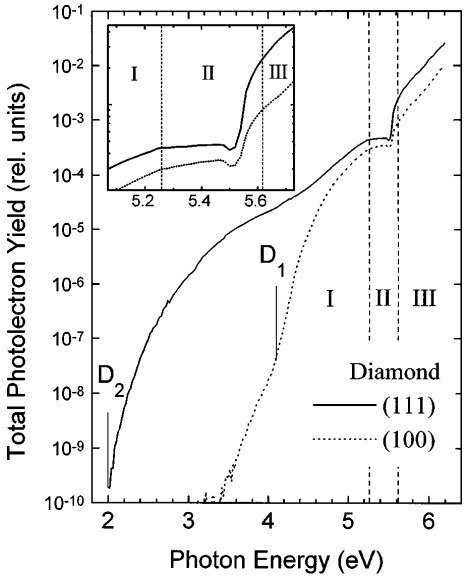

FIG. 1. Total photoelectron yield spectra of a single crystal type IIb diamond (111) and (100) surfaces after microwave hydrogenation at 850 °C. The sharp increase at 5.54 eV marks the exciton absorption edge and proves the NEA of the surfaces.

Surprisingly, however, also sub-band-gap illumination in region I can produce photoelectrons in diamond which can be due only to the excitation of electrons from defect states in the gap. Two clearly resolved thresholds at 4.1 ± 0.1 eV (D_1) and at 2.0 ± 0.1 eV (D_2) mark the onset of transitions from these defect levels to the CBM. While D_1 is present in both samples with comparable strength D_2 is significant only in the (111) crystal and, at best, indicated by a weak tail below 4.0 eV in the (100) sample. In an annealing study of heteroepitaxial diamond films deposited by chemical vapor deposition on Si(100) substrates D_1 was found to be present independent of thermal treatment [11]. A second defect close to D_2 (2.2 eV) was absent in the as deposited state of the films but could be thermally induced and reached a comparable strength as in the spectrum of the (111) crystal in Fig. 1 after annealing at 1000 °C.

With a bulk Fermi level position at 0.3 eV and a surface Fermi level at 0.9 ± 0.2 eV above the valence band maximum a moderate downward band bending of 0.6 ± 0.2 eV for our p-type IIb diamonds results, but photoelectric emission from defect states 2.0 eV below the CBM is in obvious conflict with the Fermi statistics. This indicates that the defect states are not in thermal equilibrium but optically pumped by the photoyield probe light, a complication unavoidable for defect spectroscopy in wide band gap semiconductors. Nevertheless, excitation from defects provides an unambiguous contribution of free electrons to the yield spectrum.

We now turn to region II which is shown together with part of region I on an extended scale in Fig. 2. This is the region where electrons from defect excitation and exciton absorption contribute both to the yield. But unlike

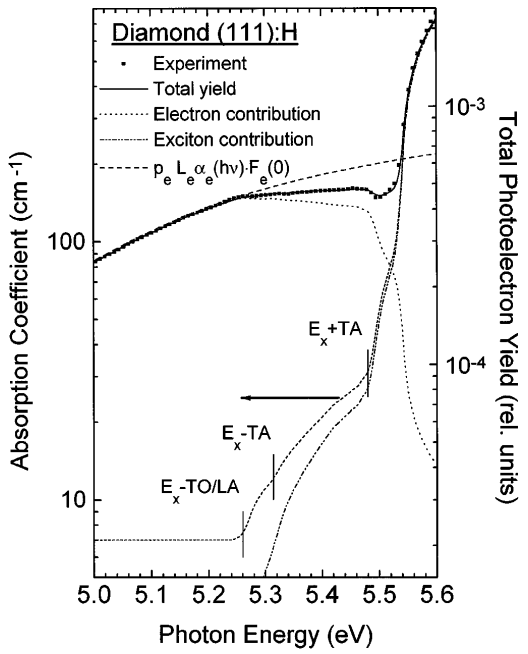

FIG. 2. Fit of the total yield spectrum of the diamond (111) sample in the band edge region based on the competition between excitation of excitons and conduction band electrons out of defects. The four square root shape thresholds in the absorption spectrum are identified with phonon replicas according to Ref. [10]. The mark at 5.53 eV corresponding to E_x + TO/LA has been omitted in the plot for clarity. For details, see text.

regions I and III where the yield follows the absorption coefficient α according to Eq. (3) it deviates here considerably from the absorption spectrum and even exhibits a pronounced local minimum around 5.5 eV that requires explanation. The absorption coefficient as measured for our samples is also plotted in Fig. 2 as the short dashed line and is referred to the left hand logarithmic scale. The constant value of 7 cm^{-1} is due to the defect absorption. At 5.26 eV exciton absorption sets in with a phonon replica involving the simultaneous absorption of an LA or TO phonon (not distinguishable) and a second, weaker square root threshold at 5.32 eV corresponds to TA phonon absorption [10]. The absorption spectrum then rises in two large steps at 5.48 and 5.53 eV as the exciton absorption is accompanied by the emission of phonons.

In order to model the simultaneous emission of free conduction band electrons after defect excitation and of electrons stemming from excitons after breakup we extend the one dimensional diffusion model of Eq. (3) in the same way as Bandis and Pate [3,4] did for region III:

$$Y(h\nu) = Y_e(h\nu) + Y_x(h\nu) = \frac{p_e L_e \alpha_e(h\nu)}{1 + L_e\alpha(h\nu)} + \frac{p_x L_x \alpha_x(h\nu)}{1 + L_x\alpha(h\nu)}. \quad (4)$$

The indices x and e refer to exciton and free electron excitation, respectively. Note that the denominators in (4) involve the total absorption constant $\alpha(h\nu) = \alpha_e(h\nu) + \alpha_h(h\nu) + \alpha_x(h\nu)$ which is a sum of three partial absorption constants due to the generation of electrons out of defects, of holes out of defects, and of excitons, respectively. $\alpha_h(h\nu)$ is not relevant for photoelectron emission but does contribute to the absorption constant. The constant absorption coefficient of 7 cm^{-1} below 5.26 eV can thus serve only as an upper limit for $\alpha_e(h\nu)$. Since in region I $L_e\alpha \ll 1$ is certainly a save approximation (in view of $\alpha \leq 7$ cm^{-1}), $Y(h\nu) \approx p_e L_e \alpha_e(h\nu)$.

Without any new absorption channel the photoyield is expected to follow the extrapolation of the defect contribution as indicated by the dashed line in Fig. 2. The break in the measured photoelectron yield away from this extrapolation at 5.26 eV and the even more pronounced minimum at 5.5 eV coincide with the onset of strong excitonic transitions. The fact that the yield drops despite the opening of new excitation channels can mean only that the exciton creation is less efficient in providing photoelectrons than the direct excitation of free conduction band electrons out of defects. A fit of the yield spectrum in terms of the absorption spectrum and based on an extension of Eq. (4) with p_e, L_e, p_x, and L_x as energy independent parameters is shown as the solid line in Fig. 2. The extension of the semi-infinite diffusion model is necessary to account for the finite thickness of the sample and will be discussed below. Since it does not modify the essential physics of the process we shall discuss the fit results in the framework of the more instructive equation (4).

The dotted and dash-dotted lines in Fig. 2 show separately the contributions $Y_e(h\nu)$ of electrons excited out of defects and $Y_x(h\nu)$ due to excitons to the total yield. With the onset of exciton absorption the generation profile (of both conduction band electrons and excitons) becomes sharper and when α exceeds significantly the inverse diffusion length L_e^{-1} of the electrons, $Y_e(h\nu)$ is effectively quenched. Simultaneously, the exciton mediated yield contribution $Y_x(h\nu)$ increases, albeit with a much smaller prefactor $p_x L_x$ as compared to the electrons. Only when α reaches 100 cm^{-1} is the loss in direct electron emission compensated by the electrons emitted as a consequence of exciton absorption and the spectral shape of the total yield finally follows perfectly the absorption constant $\alpha(h\nu) \approx \alpha_x(h\nu)$. It is evident from Eq. (4) that this agreement up to 5.6 eV where $\alpha \approx 700$ cm^{-1} implies that $L_x \ll 1/700$ cm $= 14$ μm and this limit can be set more restrictive to $L_x < 5$ μm by the fit.

From the value of the absorption constant (50 cm^{-1}) at which the electron contribution drops sharply and at which the local minimum in the yield spectrum is observed an estimate of $L_e \approx 1/50$ cm follows directly. The fit shown in Fig. 2 is indeed very sensitive to this parameter which can be fixed at $L_e = 230 \pm 20$ μm.

The yield spectrum is dominated by $Y_x(h\nu)$ above 5.54 eV. In order to fit the local minimum and the

subsequent increase of $Y(h\nu)$ with $\alpha(h\nu)$, the magnitude of $Y_x(h\nu) \approx p_x L_x \alpha_x(h\nu)$ has to be appropriately matched to $Y_e(h\nu)$ which scales with $p_e L_e \alpha_e(h\nu)$ (in region I). Because L_e is fixed by the fit and $p_e \leq 1$ and $\alpha_e \leq 7\ \mathrm{cm}^{-1}$ an upper limit of $p_x L_x \leq 0.1\ \mu\mathrm{m}$ can be extracted from our analysis.

Although a fit of the photoyield spectra on the basis of Eq. (4) and the experimentally obtained absorption spectrum would already give convincing agreement, the electron diffusion length of $230\ \mu\mathrm{m}$ necessitates the extension of the semi-infinite model because $L_e = 230 \pm 20\ \mu\mathrm{m}$ is comparable to the thickness of our samples of $d = 250\ \mu\mathrm{m}$. In fact, we carefully excluded the trivial explanation of our yield spectra, namely, that emission from the backside of our sample produced the signature discussed above simply because the light does no longer reach the backside with increasing absorption constant. For a control experiment we glued the sample tightly on a metal sample holder with conducting carbon in order to prevent electron emission from the backside; no change was observed in the photoyield spectra. Routinely samples were clamped to a tantalum sample holder. For the extension of the diffusion model to finite sample thickness we therefore assumed that a fraction R of the light was reflected from the backside of the sample and the sample holder and traveled through the sample again. This modifies the excitation profile $g(x)$ and also the probability function $w(x)$ in the following way [9]:

$$w(x) = p\,\frac{\exp(-L^{-1}d) + B\exp[-L^{-1}(2d - x)]}{1 - B^2\ \exp(2L^{-1}d)}. \quad (5)$$

The parameter $B = [1 - (S_{\mathrm{em}} + S_{\mathrm{rec}})/(L^{-1}D)]/[1 + (S_{\mathrm{em}} + S_{\mathrm{rec}})/(L^{-1}D)]$ depends on the ratio of the (generalized) recombination velocity $S = S_{\mathrm{em}} + S_{\mathrm{rec}}$ of the two surfaces and the "diffusion velocity" D/L. It varies between $+1$ for small and -1 for large surface recombination velocity. Integrating the probability function again over the excitation profile gives a correction factor $F_e(\alpha(h\nu)L_e)$ by which the yield contribution $Y_e(h\nu)$ in Eq. (4) has to be multiplied to take the finite sample thickness d into account. [In principle $Y_x(h\nu)$ must be modified correspondingly with respect to $w_x(x)$ which is, however, ineffective because $L_x \ll d$ still holds for the excitons.] F_e is a function of the (normalized) absorption constant with R, d, and B as parameters. The fit in Fig. 2 was performed taking $R = 0.48$ for our tantalum sample holder [12] and $B = 0$, i.e., $S = L^{-1}D$, and gave $L_e = 230 \pm 20\ \mu\mathrm{m}$. For the extreme case of $S \ll L^{-1}D$, i.e., $B = 1$, a comparable agreement between the model and the experiment was achieved with $L_e = 175 \pm 25\ \mu\mathrm{m}$, whereas for $S > 3L^{-1}D$ the fit considerably degrades and the local minimum in the yield spectrum can no longer be reproduced.

The large diffusion length resulting for the minority carriers in our natural diamonds might at first glance be surprising. One must keep in mind, however, that these specimens are very pure containing an acceptor concentration of the order of $10^{16}\ \mathrm{cm}^{-3}$ and even less compensating nitrogen impurities. Their impurity concentration is comparable to crystalline p-type silicon grown by the Czochalsky method for which similar diffusion lengths have been reported [13].

In summary, new photoelectron yield experiments with high dynamical range on diamond (100) and (111) surfaces exhibiting NEA revealed new channels for electron emission based on bulk defect absorption. Two defect levels at 2.0 ± 0.1 and 4.1 ± 0.1 eV below the conduction band minimum were identified from the spectra. A quantitative fit of the yield spectra was performed in the region where defect and exciton absorption interfere to give a highly structured spectrum. From the fit we derive the electron diffusion length in type IIb diamond and an upper limit for the exciton diffusion length which is smaller by a factor of 30.

[1] F. J. Himpsel, J. A. Knapp, J. A. Van Vechten, and D. E. Eastman, Phys. Rev. B **20**, 624 (1979).
[2] J. Van der Weide, Z. Zhang, P. K. Baumann, M. G. Wensell, J. Bernholc, and R. J. Nemanich, Phys. Rev. B **50**, 5803 (1994).
[3] C. Bandis and B. B. Pate, Phys. Rev. Lett. **74**, 777 (1995).
[4] C. Bandis and B. B. Pate, Phys. Rev. B **52**, 12 056 (1995).
[5] J. Schäfer, J. Ristein, L. Ley, and H. Ibach, Rev. Sci. Instrum. **64**, 653 (1993).
[6] B. D. Thoms, M. S. Owens, J. E. Butler, and C. Spiro, Appl. Phys. Lett. **65**, 2957 (1994).
[7] O. M. Küttel, K. Diederich, E. Schaller, O. Carnal, and L. Schlapbach, Surf. Sci. **337**, L812 (1995).
[8] P. T. Wedepohl, Proc. Phys. Soc. **52**, 177 (1957).
[9] R. L. Bell, *Negative Electron Affinity Devices* (Clarendon, Oxford, 1973), p. 24ff.
[10] C. C. Clark, P. J. Dean, and P. V. Harris, Proc. R. Soc. London A **277**, 312 (1964).
[11] W. Stein, J. Ristein, and L. Ley (to be published).
[12] J. H. Weaver, D. W. Lynch, and C. G. Olson, Phys. Rev. B **10**, 501 (1974).
[13] L. Passari and E. Susi, J. Appl. Phys. **54**, 3935 (1983).